Effect of Lanthanide Element on Glass-Forming Ability and Local Atomic Structure of Fe-Co-(Ln)-B Amorphous Alloys

Materials Transactions, JIM, Vol. 40, No. 10 (1999), pp. 1144 to 1148

Effect of Lanthanide Element on Glass-Forming Ability and Local Atomic Structure of Fe–Co–(Ln)–B Amorphous Alloys

Muneyuki Imafuku*, Kenichi Yaoita*, Shigeo Sato*, Wei Zhang* and Akihisa Inoue**

*Inoue Superliquid Glass Project, Exploratory Research for Advanced Technology, Japan Science and Technology Corporation, Sendai 982-0807, Japan
**Institute for Materials Research, Tohoku University, Sendai 980-8577, Japan

The glass-forming ability and the local ordering structures of $Fe_{70}Co_{10}B_{20}$ and $Fe_{67}Co_{10}Ln_3B_{20}$ (Ln=Sm, Tb or Dy) alloys have been studied by differential scanning calorimetry (DSC), density measurement and X-ray diffraction method. The supercooled liquid region, defined by the temperature interval ΔT_x between glass transition temperature T_g and onset crystallization temperature T_x, appears and is extended by the addition of lanthanide element in Fe–Co–B systems. ΔT_x ($\Delta T_x = T_x - T_g$) is 32 K for $Fe_{67}Co_{10}Sm_3B_{20}$, 36 K for $Fe_{67}Co_{10}Tb_3B_{20}$ and 38 K for $Fe_{67}Co_{10}Dy_3B_{20}$. The packing fraction, defined by the ratio of total volume of atoms to the volume of a cell, increases by a few percent in these alloys. The least-squares refining analysis for interference functions as well as the usual radial distribution function analysis shows that the coordination number of transition metals around Fe decreases by the addition of the lanthanide element whereas the change in the coordination number of transition metals around B is not clearly observed within the experimental uncertainty. The lanthanide element is considered to play an important role in forming a dense packing structure so as to rearrange the network of local ordering units of (Fe, Co)–B in these alloys.

(Received May 20, 1999; In Final Form August 24, 1999)

Keywords: *iron-based amorphous alloy, glass transition, supercooled liquid region, iron-cobalt-lanthanide metal-boron system, packing fraction, X-ray diffraction, local atomic structure*

I. Introduction

Ferrous amorphous alloys with large glass-forming ability and good soft magnetic properties have been found in a number of multicomponent systems such as Fe–(Al, Ga)–(P, C, B, Si)[1][2], Fe–(Nb, Mo)–(Al, Ga)–(P, B, Si)[3], Fe–(Co, Ni)–Zr–B[4][5], Fe–(Co, Ni)–(Zr, Nb)–(Mo, W)–B[6]. As pointed out by Inoue[7]-[9], these alloy systems satisfy three empirical rules of the constituents, *i.e.*, (1) the multicomponent system consisting of more than three elements, (2) the different atomic size ratios beyond about 12% among the main component, (3) the negative heats of mixing among their elements. Within the framework of these empirical rules, Zhang and Inoue[10] have recently reported new quaternary Fe–Co base amorphous alloys, Fe–Co–(Nd, Sm, Tb, Dy)–B, with supercooled liquid region by adding lanthanide elements with relatively large atomic size to ternary Fe–Co–B systems. Amorphous $Fe_{80-x-y}Co_xLn_yB_{20}$ (Ln=Sm or Tb, x=0 to 10 at%, y=1.5 to 3.0 at%) alloys are found to provide large magnetostriction (λ_s) values of $37\text{–}58 \times 10^{-6}$ combined with good bending ductility, high tensile fracture strength exceeding 3000 MPa. However, there is no information about the local atomic structures of these particular alloys, which should be closely related to the origin of their large glass-forming ability.

The main purpose of this paper is to present the local atomic structure of amorphous $Fe_{70}Co_{10}B_{20}$ and $Fe_{67}Co_{10}Ln_3B_{20}$ (Ln=Sm, Tb or Dy) alloys with special reference to the effect of lanthanide element on their glass forming ability.

II. Experimental

$Fe_{70}Co_{10}B_{20}$, $Fe_{67}Co_{10}Sm_3B_{20}$, $Fe_{67}Co_{10}Tb_3B_{20}$ and $Fe_{67}Co_{10}Dy_3B_{20}$ alloy ingots were prepared from the mixture of pure metals and pure boron crystal by arc melting in an argon atmosphere. Rapidly solidified amorphous ribbons of about 0.02 mm thick and 1.5 mm wide were prepared by the single-roller melt spinning technique from their alloy ingots. Thermal stability was examined by differential scanning calorimetry (DSC) at a heating rate of 0.67 K/s. Densities of samples were measured by Archimedean method with toluene. The average number density of each sample was evaluated from its composition and density.

X-ray diffraction method was employed for obtaining the atomic structures of amorphous alloys. The experimental procedure was almost identical to the previous works on amorphous alloys[11]-[13]. Thus, only some essential points and additional details, which are necessary for the present work, are given below. Scattered X-ray intensities measured by monochromatic Mo K_α radiation were corrected for air scattering, absorption and polarization, and converted to electron units per atom with the generalized Krogh-Moe-Norman method[11] us-

ing the X-ray scattering factors with anomalous dispersion terms[14] and the theoretically-calculated Compton scattering values[15]. Interference function $Qi(Q)$ can be estimated from the coherent scattering intensity $I_{coh}(Q)$ in electron unit per atom as

$$Qi(Q)=Q\frac{I_{coh}(Q)-\Sigma c_j f_j^2}{(\Sigma c_j f_j)^2} \quad (1)$$

where c_j and f_j are the atomic concentration and the scattering factor of element j, respectively. The Fourier transformation of $Qi(Q)$ in eq. (1) gives the radial distribution function (RDF), $2\pi^2 r\rho(r)$ as follows;

$$2\pi^2 r\rho(r)=2\pi^2 r\rho_0+\int_0^{Q_{max}} Qi(Q)\sin(Qr)\,dQ \quad (2)$$

where ρ_0 and Q_{max} are the average number density in the system and the maximum value of wave vector Q, respectively. In this work, Q_{max} was selected to be 150 nm^{-1}, which was considered to be large enough not to give serious truncating effect in Fourier transformation[11]. The least-squares variation method[16][17] for the interference functions was used to determine the local structure parameters; coordination numbers and interatomic distances for the neighboring pairs. This variational method is to use the assumption that the interference function can be represented by a discrete Gaussian distribution in near neighbor region and a continuous distribution with an average number density at long distance.

III. Results and Discussion

Glass-forming ability can be estimated by temperature interval between the glass transition temperature T_g and onset crystallization temperature T_x, ΔT_x ($\Delta T_x=T_x-T_g$)[18]. Generally, the larger temperature interval ΔT_x represents the higher glass-forming ability. **Figure 1** shows the DSC curves of the melt spun $Fe_{70}Co_{10}B_{20}$ and $Fe_{67}Co_{10}Ln_3B_{20}$ (Ln=Sm, Tb or Dy) amorphous ribbons. For ternary alloy system of $Fe_{70}Co_{10}B_{20}$, T_g is not observed and the amorphous state directly changes to crystalline state upon heating. On the other hand, the quaternary $Fe_{67}Co_{10}Ln_3B_{20}$ (Ln=Sm, Tb or Dy) alloys exhibit the glass transition, followed by the appearance of a supercooled liquid region and then crystallization. The values of T_x, T_g and ΔT_x are 830, 798 and 32 K, respectively, for $Fe_{67}Co_{10}Sm_3B_{20}$. Similarly, 831, 795 and 36 K, for $Fe_{67}Co_{10}Tb_3B_{20}$ and 841, 803 and 38 K, for $Fe_{67}Co_{10}Dy_3B_{20}$. It may be also worthy of notice that larger ΔT_x values of 45 to 85 K were found in other new multicomponet ferrous alloys of $Fe_{56}Co_7Ni_7Zr_{10-x}Nb_xB_{20}$ (x=0 to 10 at%) systems[19]. It is remarkable, however, that only a small amount of lanthanide element induces to appear the supercooled liquid region.

The density values were determined as 7.42 Mg/m^3 for $Fe_{70}Co_{10}B_{20}$, 7.68 Mg/m^3 for $Fe_{67}Co_{10}Sm_3B_{20}$, 7.68 Mg/m^3 for $Fe_{67}Co_{10}Tb_3B_{20}$ and 7.71 Mg/m^3 for $Fe_{67}Co_{10}Dy_3B_{20}$ amorphous alloys, respectively. The

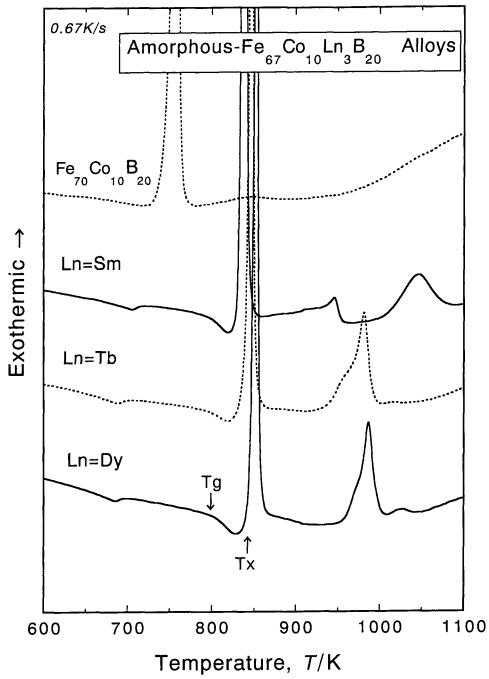

Fig. 1 The DSC curves of $Fe_{70}Co_{10}B_{20}$, $Fe_{67}Co_{10}Sm_3B_{20}$, $Fe_{67}Co_{10}Tb_3B_{20}$ and $Fe_{67}Co_{10}Dy_3B_{20}$ amorphous alloys.

density value of $Fe_{70}Co_{10}B_{20}$ amorphous alloy is on the extraporated value between those of amorphous $Fe_{80}B_{20}$ and $Co_{80}B_{20}$[20]. As is expected, the density of $Fe_{70}Co_{10}B_{20}$ amorphous alloy increases when adding a relatively heavy lanthanide element. The number densities ρ_0 in eq. (2) were calculated to be 94.8, 92.1, 92.5 and 92.2 atoms/nm^3 for $Fe_{70}Co_{10}B_{20}$, $Fe_{67}Co_{10}Sm_3B_{20}$, $Fe_{67}Co_{10}Tb_3B_{20}$ and $Fe_{67}Co_{10}Dy_3B_{20}$ amorphous alloys, respectively. This implies that the number of atoms per unit volume decreases by the addition of a relatively large lanthanide element. Considering many factors such as the empirical rules described in Section I and small change in density upon crystallization[21], amorphous phase with a structure of nearly dense random packing structure is likely to be formed in multicomponent alloy system with the supercooled liquid region. Let us suppose the simple rigid hard sphere model[22] in which constituent atoms are randomly packed as hard spheres. Then, we can estimate the packing fraction, defined by the ratio of total volume of atoms to the volume of a cell, in these amorphous alloys by using the atomic radii of constituents and the number density. The resultant packing fractions of $Fe_{67}Co_{10}Sm_3B_{20}$ are 0.745, 0.746 for $Fe_{67}Co_{10}Tb_3B_{20}$ and 0.742 for $Fe_{67}Co_{10}Dy_3B_{20}$, respectively. These values are slightly higher than that of $Fe_{70}Co_{10}B_{20}$, 0.722. Increase in the packing fraction, in a sense of the first order approximation, suggests that an addition of relatively large lanthanide element to $Fe_{70}Co_{10}B_{20}$ modifies the local ordering structure to more dense packed amorphous alloys. Further study is strongly required to discuss the degree of dense random packing structure for amorphous alloys in detail, because the occupation volume or the free volume in solids de-

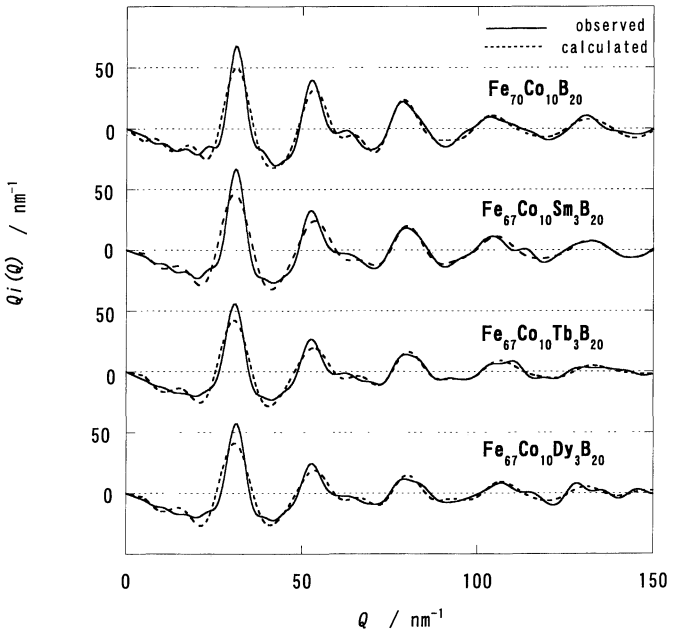

Fig. 2 Interference functions of $Fe_{70}Co_{10}B_{20}$, $Fe_{67}Co_{10}Sm_3B_{20}$, $Fe_{67}Co_{10}Tb_3B_{20}$ and $Fe_{67}Co_{10}Dy_3B_{20}$ amorphous alloys. The solid and dotted curves correspond to the experimental and calculated ones. The calculation was done by the least-squares variation method.

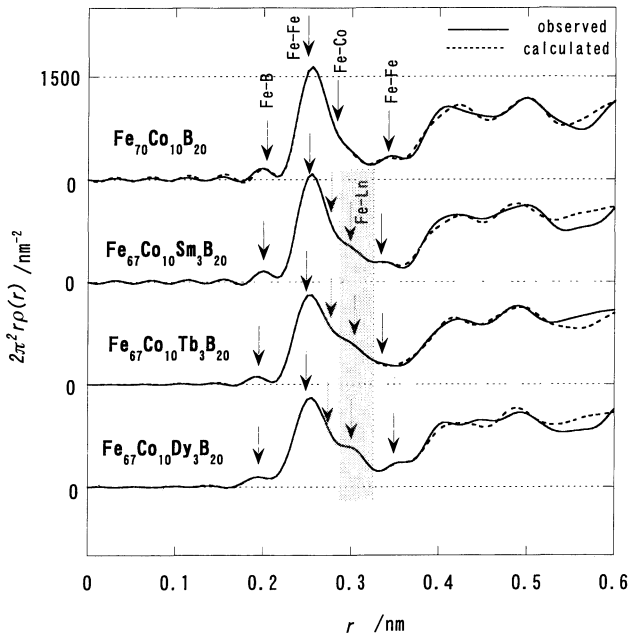

Fig. 3 Radial distribution functions (RDFs) of $Fe_{70}Co_{10}B_{20}$, $Fe_{67}Co_{10}Sm_3B_{20}$, $Fe_{67}Co_{10}Tb_3B_{20}$ and $Fe_{67}Co_{10}Dy_3B_{20}$ amorphous alloys. The solid and dotted curves correspond to the experimental and calculated ones. The calculation was done by the least-squares variation method. Inserted arrows indicate the calculated interatomic distances together with the atomic pairs.

pends not only on the chemical composition but also on the electronic properties of constituents.

The experimental and calculated interference functions $Qi(Q)$ of $Fe_{70}Co_{10}B_{20}$ and $Fe_{67}Co_{10}Ln_3B_{20}$ (Ln=Sm, Tb or Dy) amorphous alloys are shown in **Fig. 2**. A shoulder in the second peak of $Qi(Q)$ around $Q=60\,nm^{-1}$ is clearly observed for $Fe_{70}Co_{10}B_{20}$. This is the characteristic feature of various amorphous alloys[23] and this may be, more or less, attributed to the existence of a certain structural ordering. In transition metal-metalloid amorphous alloys, especially for the Fe-B system, amorphous structures are classified into two types, *i.e.*, Bernal type and chemical order type by their composition[24]. When boron content is larger than 18% in Fe-B system, the chemical order type structure characterized by the local ordering units of A_3B or A_2B becomes dominant. The stereo-chemical model with the network structure of trigonal prismatic unit of A_6B observed in the orthorhombic phase of Fe_3C has also been proposed in these alloys[25][26]. Same as for the binary $Fe_{80}B_{20}$ system, the local ordering is quite likely to exist in $Fe_{70}Co_{10}B_{20}$ by exchanging some amount of Fe to Co. It is distinct that the shoulder in the second peak becomes weak but still remains in the $Qi(Q)$ profiles of quaternary amorphous alloys, $Fe_{67}Co_{10}Ln_3B_{20}$ (Ln=Sm, Tb or Dy). This contrasts with the fact that the characteristic shoulder in the second peak is not observed at all in Pt-Ni-P[27], Pt-P[28] and La-Al-Ni[29] amorphous alloys. The constituent atoms in these alloys are considered to be randomly and homogeneously mixed like liquid with good harmony of the large difference in atomic size and chemical affinity among constituents. This feature suggests that the addition of lanthanide element with large atomic size reduce the atomic ordering of $Fe_{70}Co_{10}B_{20}$ by breaking the network structure of the local ordering units of $Fe_{70}Co_{10}B_{20}$.

Radial distribution functions calculated from the Fourier transformation of the interference functions by eq. (2) are shown in **Fig. 3**. The split in the second peak at $r=0.4$–0.5 nm seems to be slightly obscure when adding a small amount of lanthanide element to the $Fe_{70}Co_{10}B_{20}$ base alloy, although the main structural profile of RDFs is unchanged. Such behavior may correspond to the variation detected in $Qi(Q)$. For convenience of discussion for the amorphous structures, coordination number N_{ij} and inter-atomic distances r_{ij} for the neighboring pairs of type-i and type-j atoms were calculated to reproduce the $Qi(Q)$ profiles by the least-squares variation method. The dotted lines in Figs. 2 and 3 show the fitted curves of $Qi(Q)$ and resultant RDFs, respectively. Arrows in Fig. 3 indicate the main possible interatomic distances and types of pairs taken into account. Obtained structural parameters with respect to the environment around Fe are summarized in Table 1. Significant change in structural parameters of Fe-Fe pairs is clearly seen from this table. The coordination numbers of Fe-Fe pairs for $Fe_{67}Co_{10}Ln_3B_{20}$ (Ln=Sm, Tb or Dy) at the first peak is much less than that for $Fe_{70}Co_{10}B_{20}$. Besides, the interatomic distance becomes slightly shorter for $Fe_{67}Co_{10}Ln_3B_{20}$ (Ln=Sm, Tb or Dy). The variation in the Fe-B correlation, on the other hand, dose not show a clear tendency when adding lanthanide element.

Table 1 Summary of coordination numbers and interatomic distances for $Fe_{70}Co_{10}B_{20}$, $Fe_{67}Co_{10}Sm_3B_{20}$, $Fe_{67}Co_{10}Tb_3B_{20}$ and $Fe_{67}Co_{10}Dy_3B_{20}$ amorphous alloys.

	Fe-B		Fe-Fe		Fe-Co		Fe-Ln	
	r/nm	N/atom	r/nm	N/atom	r/atom	N/atom	r/nm	N/atom
$Fe_{70}Co_{10}B_{20}$	0.205±0.005	2.0±0.4	0.252±0.001	7.8±0.2	0.281±0.001	1.8±0.1	—	—
$Fe_{67}Co_{10}Sm_3B_{20}$	0.205±0.004	2.2±0.5	0.248±0.000	6.4±0.2	0.266±0.001	2.6±0.1	0.296±0.001	0.6±0.0
$Fe_{67}Co_{10}Tb_3B_{20}$	0.197±0.004	1.6±0.4	0.246±0.001	6.5±0.3	0.272±0.001	2.7±0.1	0.305±0.001	0.7±0.0
$Fe_{67}Co_{10}Dy_3B_{20}$	0.198±0.003	2.7±0.4	0.243±0.001	5.4±0.4	0.268±0.001	3.0±0.1	0.303±0.001	0.7±0.0

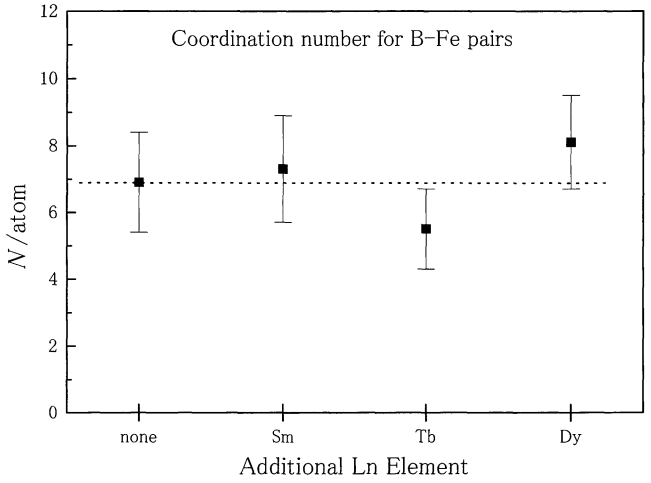

Fig. 4 Comparison of coordination numbers of B-Fe pairs for $Fe_{70}Co_{10}B_{20}$, $Fe_{67}Co_{10}Sm_3B_{20}$, $Fe_{67}Co_{10}Tb_3B_{20}$ and $Fe_{67}Co_{10}Dy_3B_{20}$ amorphous alloys. Dotted line represents the level of $Fe_{70}Co_{10}B_{20}$.

Structural parameters for the environment around B were calculated in order to facilitate the understanding of the trigonal prismatic units of Fe_6B proposed in various Fe-B based amorphous alloys. **Figure 4** shows the comparison of coordination numbers of B-Fe pairs for $Fe_{70}Co_{10}B_{20}$ and $Fe_{67}Co_{10}Ln_3B_{20}$ (Ln=Sm, Tb or Dy) with the experimental uncertainty. The values of N_{BFe}s for all amorphous alloys are dispersed around 6.0, of which value is found in trigonal prism of Fe_6B. Thus, it is safely concluded that the same kind of local ordering structure as in trigonal prismatic units of $(Fe, Co)_6B$ in $Fe_{70}Co_{10}B_{20}$ still remains in $Fe_{67}Co_{10}Ln_3B_{20}$ (Ln=Sm, Tb or Dy). Once the disordered network of local structural unit of $(Fe, Co)_6B$ is formed, lanthanide elements are too large to squeeze in each unit. These elements rather stay in between such local ordering units to slightly rearrange their network structure. This is consistent with the following observation. As these units are connected mainly with Fe atoms, the correlation of Fe-Fe pairs becomes week and its coordination number decreases by the addition of lanthanide element.

When adding lanthanide element to $Fe_{70}Co_{10}B_{20}$, the distance of Fe-Fe pair decreases. This experimental fact for $Fe_{67}Co_{10}Ln_3B_{20}$ (Ln=Sm, Tb or Dy) alloys suggest that the degree of atomic packing increases compared with that of ternary $Fe_{70}Co_{10}B_{20}$ alloy.

IV. Concluding Remarks

The effect of lanthanide element such as Sm, Tb or Dy on the glass forming ability and the variation of local ordering structures of amorphous Fe-Co-(Ln)-B systems have been studied by differential scanning calorimetry (DSC), density measurement and X-ray diffraction. It is known that an addition of small amount of lanthanide element induces the appearance of supercooled liquid region in Fe-Co-B system. ΔT_x ($\Delta T_x = T_x - T_g$) ranges from 32 to 38 K in these alloys. A few percent increase of packing fraction is observed as predicted in the Inoue's empirical rules[7]-[9]. The coordination number of transition metals around Fe decreases by the addition of lanthanide element whereas the change in the coordination number of transition metals around B is not clearly observed within the experimental uncertainty. These features are explained by the disordered network model with trigonal prism-like local ordering structure of (Fe, Co)-B. Lanthanide element plays an important role in forming the dense random packing structure of (Fe, Co)-B in these alloys. However, some further experimental studies, particularly the environmental structure around lanthanide element, should be required before the full potential of the present conclusion can be assessed.

Acknowledgement

The authors would like to thank Associate Professor E. Matsubara of Kyoto University, Japan and Professor Y. Waseda of Tohoku University, Japan for useful discussion.

REFERENCES

(1) A. Inoue and J. S. Gook: Mater. Trans., JIM, **36** (1995), 1180-1183.
(2) A. Inoue, A. Takeuchi T. Zhang, A. Murakami and A. Makino: IEEE Trans. Magn., **32** (1996), 4866-4871.
(3) A. Inoue and J. S. Gook: Mater. Trans., JIM, **37** (1996), 32-38.
(4) A. Inoue and T. Zhang, T. Itoi and A. Takeuchi: Mater. Trans., JIM, **38** (1997), 359-362.
(5) A. Inoue and H. Koshiba: Appl. Phys. Lett., **37** (1998), 744-746.
(6) A. Inoue, T. Zhang and A. Takeuchi: Appl. Phys. Lett., **71** (1997), 464-466.
(7) A. Inoue: Mater. Sci. Forum, **179-181** (1995), 691-700.
(8) A. Inoue: Sci. Rep. Res. Inst. Tohoku Univ., **A42** (1996), 1-11.
(9) A. Inoue: Mater. Trans., JIM, **36** (1995), 866-875.
(10) W. Zhang and A. Inoue: Mater. Trans. JIM, **40** (1999), 78-81.
(11) Y. Waseda: *The Structure of Non-Crystalline Materials*, MacGraw-Hill, New York, (1980), pp. 27-51 and pp. 87-132.

(12) E. Matsubara, T. Zhang and A. Inoue: Sci. Rep. Res. Inst. Tohoku Univ., **A43** (1997), 83–87.
(13) C. Park, M. Saito, A. Takeuchi, A. Inoue and Y. Waseda: High Temp. Mater. & Processes, **16** (1997), 57–64.
(14) *International Tables for X-ray Crystallography Vol. IV*, ed. J. A. Ibers and W. C. Hamilton, Kynoch Press, Birmingham, (1974), pp. 71–102 and pp. 148–151.
(15) D. T. Cromer: J. Chem. Phys., **50** (1969), 4857–4859.
(16) A. H. Narten and H. A. Levy: Science, **165** (1969), 447–454.
(17) A. H. Narten: J. Chem. Phys., **56** (1972), 1905–1909.
(18) Y. Li, S. C. Ng, C. K. Ong, H. H. Hng and T. T. Goh: Scripta Mater., **36** (1997), 783–787.
(19) A. Inoue, H. Koshiba, T. Zhang and A. Makino: Mater. Trans. JIM, **38** (1997), 577–582.
(20) K. Shirakawa, Y. Waseda and T. Masumoto: Sci. Rep. Res. Inst. Tohoku Univ., **A29** (1981), 229–239.
(21) A. Inoue: Mater. Sci. Forum, **269–272** (1998), 855–864.
(22) J. D. Bernal: Nature, **183** (1959), 141–147.
(23) Y. Waseda: Solid State Physics, **10** (1975), 459–474 [in Japanese].
(24) Y. Waseda and H. S. Chen: Sci. Rep. Res. Inst. Tohoku Univ., **A28** (1981), 143–155.
(25) P. H. Gaskell: J. Non-Cryst. Solids, **32** (1979), 207–224.
(26) P. H. Gaskell: J. Non-Cryst. Solids, **75** (1985), 329–346.
(27) A. Shinha and P. Duwez: J. Phys. Chem. Solids, **32** (1971), 267–277.
(28) H. S. Chen, Y. Waseda and K. T. Aust: Phys. Stat. Sol., **a65** (1981), 695–700.
(29) E. Matsubara, T. Tamura, Y. Waseda, T. Zhang, A. Inoue and T. Masumoto: J. Non-Cryst. Solids, **150** (1992), 380–385.